International Journal of Wireless Information Networks
https://doi.org/10.1007/s10776-021-00540-9

Spatial–Temporal Fusion Based Path Planning for Source Seeking in Wireless Sensor Network

Cheng Xu[1,2] · Jiawei Rong[1] · Yulin Chen[1] · Hang Wu[1] · Shihong Duan[1]

Received: 6 February 2021 / Revised: 2 June 2021 / Accepted: 22 October 2021

Abstract
Source seeking problem has been faced in many fields, especially in search and rescue applications. We proposed a virtual structure-based spatial–temporal method to realize cooperative source seeking using multi-agents. Spatially, a circular formation is considered to gather collaborative information and estimate the gradient direction of the formation center. In terms of temporal information, we use the formation positions in time sequence to construct a virtual structure sequence. Then, we fuse the sequential gradient as a whole. Experimental results show that, compared with state-of-the-art, the proposed method can quickly and efficiently find the source so that the formation can minimize the movement distance during the moving process and increase the efficiency of source seeking. Numerical simulations confirm the efficiency of the scheme put forth. Compared with state-of-the-art source-seeking methods, the iterative steps of our proposed method are reduced by 20%, indicating that the method can find the signal source with higher efficiency and lower energy consumption, and better robustness.

Keywords Cooperative computing · Gradient estimation · Source seeking · Circular formation · Spatial–temporal information

1 Introduction

1.1 Motivation

In the last decade, *cooperative source seeking* based on multi-agents (or multi-robots) has been drawing more and more attention and widely used in many fields, such as oil exploration [1], odor source search [2], environmental monitoring [3], pollution detection [4], and first-response search and rescue (SAR) tasks [5], etc. The target signal source can generally be an electromagnetic signal, an acoustic signal, or a chemical or biological signal. For example, in the event of a gas leak, rescuers need to be dispatched to find the leak source. At the same time, the lives of the participating rescuers must be protected as much as possible to avoid causing serious safety accidents. For the sake of safety and efficiency, robots (also known as agents) replace search and rescue personnel to enter dangerous areas and perform SAR operations. For example, when looking for a missing backpacker with a positioning signal device in the wild, drones or unmanned vehicles can be used to perform search and rescue missions in the face of complex terrain conditions. To sum up, a source search algorithm with higher accuracy and consistency is of practical significance in many aspects, such as industrial production, military security, and civil security (Fig. 1).

1.2 Related Work

Many existing signal source-seeking algorithms have evolved from the inspiration of biological behavior. Based on observations of spiny lobster behaviors, Consi et al. [6] proposed an agent that simulates the behavior of lobsters. In [7], inspired by silkworm moths, Kuwana et al. proposed a sourcing method that imitated the behaviors of silkworm moths seeking odor sources. Russell et al. [8] also verified

✉ Cheng Xu
xucheng@ustb.edu.cn

✉ Shihong Duan
duansh@ustb.edu.cn

[1] School of Computer and Communication Engineering, University of Science and Technology Beijing, Beijing, China

[2] Shunde Graduate School, University of Science and Technology Beijing, Beijing, China

Published online: 20 November 2021

Fig. 1 A typical application use case: multiple unmanned aerial vehicles (UAVs) work cooperatively to search the missing tour pal who carries positioning devices

the applicability of the above-mentioned algorithm to chemical source tracing in airflow environments.

However, the aforementioned biometric methods are based on the inspiration of individual biological behavior and still face obvious limitations. They rely on the information generally collected by only one single agent, such as in [6] and [7]. The individual agent lacks information interaction with other agents, making it difficult for researchers to generate it in scenarios where multiple agents work together. Although the efficiency of source-seeking methods has been improved, the limitations of single agents will lead to insufficient information collection, and low robustness [6, 7].

Many organisms in the natural world forage and reproduce through group behaviors [9–11]. Clustered organisms can efficiently find food and avoid natural enemies through the individual division of labor and information exchange. It has the characteristics of high efficiency and strong adaptability. Through the observation of biological populations, researchers proposed multiple swarm optimization algorithms, such as ant colony [9], bee colony [10], and wolf colony [11]. In 1992, Marco Dorigo [9] proposed an ant colony optimization algorithm by simulating the principles of ant social division of labor and cooperative foraging. Based on the inspiration of bee colonies to find nectar sources, Karaboga proposed the Artificial Bee Colony (ABC) [10] in 2005, which has the advantages of high accuracy and fewer control parameters. The algorithm was successfully applied to many fields such as artificial neural network training, and combination optimization [12]. In [11], Wu et al. were inspired by the cooperative hunting behavior of wolves and proposed the Wolf Pack Algorithm (WPA). The swarming behavior of fish schools has also attracted researchers' attention. In [13, 14], Wu et al. and Said the behavior of fish swarm clusters inspired Al-Abri et al. to study a cooperative, collaborative mobile strategy called *acceleration-deceleration*. It can simulate the swarm behavior of fish schools, avoiding light and move the agent team to the position of the signal source. Kennedy and Eberhart et al. [15] firstly proposed Particle Swarm Optimization (PSO), which was originally proposed to simulate the motion of bird swarms. Jatmiko et al. [16, 17] applied the particle swarm optimization algorithm to the field of odor source localization, which uses multiple agents to find stationary odor sources. Song et al. [18] proposed an improved probabilistic particle swarm optimization algorithm for source seeking in a ventilated environment. As intelligent robots and sensors work very differently from real creatures, biological behavior-inspired methods also have limitations. Besides, uncoordinated agents can cause resource competition and conflicts, which affects the overall performance of multiple agents.

Gradient-based methods are also widely considered in source-seeking applications, mainly divided into single-agent methods and multi-agents cooperative ones. As for the single agent, in [19–21], researchers used random gradient estimation to make the agent randomly move in the signal field, measure the spatial information of the signal field, and calculate the gradient direction of the signal field. Krstic et al. [19, 20] applied extreme value search control to make a single agent move to the local signal maximum in a noise-free signal field. Anatasov et al. [21] made a single agent calculate the gradient by random movement and drove the agent to signal source with gradient information. However, the above-mentioned single-target-based gradient source seeking method still faces the following main problems:

(1) Random gradient estimation can avoid local extremes to a certain extent, but the agent must constantly move back and forth to measure the signal strength to calculate the gradient.
(2) The sudden failure of the single robot may lead to the failure of the whole source seeking a task, which means a low fault tolerance and robustness.

More and more researchers are focusing on cooperative source seeking. Petter Ögren et al. [22] used a coordinated movement strategy to drive the team to the signal source by the least square method. Zhu et al. [23] utilized the leader-follower strategy combined with the least-squares to calculate the gradient direction. In [24], Li et al. used the method of least squares estimator to enable the agent team to calculate the gradient collaboratively. The method proposed by Ruggero Fabbiano et al. in [25] enables the agents to sustain a circular formation by maintaining the same relative angle and drive the agent team to the signal source with the gradient descent algorithm. In [21, 26, 27], Lara-Brinon et al. proposed a circular formation method, which enables the team to maintain a uniformly distributed circular formation, which means the agents calculate the gradient and drive themselves to the signal source.

However, the above-mentioned cooperative source-seeking methods consider the agent-formation but only use

spatial information in the signal field. They do not effectively use the information in time sequence alongside the gradient direction. Signal strength measurement and intelligent formation control will inevitably have errors. The source-seeking results obtained by gradient estimation using error signals and position information are often of poor accuracy.

1.3 Contribution and Outlines

This paper aims to propose a source-seeking method that utilizes spatial and temporal information in the scalar signal field, improving source-seeking efficiency. The main contributions could be summarized as follows.

(1) Both spatial and temporal information in source-seeking issues is taken into consideration. Spatially, a circular formation is considered to gather collaborative information and estimate the gradient direction of the formation center. In terms of temporal information, we use the formation positions in time sequence to construct a virtual structure sequence. Then, we fuse the sequential gradient as a whole. The proposed method was verified from both theoretical and numerical aspects.
(2) A control strategy with minimum movement cost is proposed. This strategy rotates the target formation by a certain angle to make the robot team achieve the minimum moving distance value when the circular team moves to the next position. Experimental results show that the proposed method can quickly find the source in as few distances as possible compared with the state-of-the-art.

The rest of this paper is organized as follows. Section 2 puts forward the specific definition of the cooperative source seeking a problem. Section 3 focuses on the details of the proposed virtual structure-based method. Carmér-Rao Lower Bound (CRLB) and Lyapunov stability analysis are presented in Sect. 4. Section 5 demonstrates the experimental verification and detailed analysis. Conclusions are drawn in Sect. 6.

2 Problem Formulation

The problem of source seeking mainly refers to the searching of signal sources in unknown scalar fields. This paper proposed a cooperative source-seeking method with the fusion of spatial and temporal information collected by agents in formation. The agents move advance along the gradient descent direction of the signal field and finally reach the position of the source.

We assume that the agent team moves in a two-dimensional space. For each agent i in the group, its dynamic equations could be denoted as follows:

$$\dot{p}_i = v_i[\cos\theta_i, \sin\theta_i]^{\mathrm{T}} \tag{1}$$

$$\dot{\theta}_i = u_i \tag{2}$$

where $p_i \in \mathbb{R}^2$ is the position vector of agent i, θ_i is the heading angle, and the control inputs are the vehicle's forward velocity v_i and turning rate u_i.

The nodes are collected into a vertex set $\mathcal{V}$, while links between nodes are collected in an edge set $\mathcal{E}$. Communication and measurements between nodes are bidirectional, so that $\Leftarrow\mathcal{V}\Leftrightarrow\mathcal{E}\Rightarrow$ forms an undirected graph $\mathcal{G}$. The agents can communicate with each other within the communication topology and generally include the following information: the coordinates, the speed, measured signal strength information, etc. For simplicity, we assume that the communication between robot pairs is bidirectional and fully connected, and any pair of agents can exchange information with each other. The performance of the proposed algorithm under limited communication conditions is not within the scope of this paper and is left for further studies.

The scalar signal field distribution function is represented as $z(p) : \mathbb{R}^2 \to \mathbb{R}$, which does not change over time. Its independent variable is coordinates of the sampling points denoted as p, and the signal strength reaches a maximum value at the source location p_s.

3 Spatial–Temporal Source Seeking

This section detailed the proposed cooperative source-seeking method, which combines the spatial and temporal information of the signal strength in the signal field. First, we give a brief introduction to the circular formation-based collective gradient estimation criterion to utilize the spatial distribution of the signal field. Then, we fuse the temporal information of the signal field by sequential sampling. Finally, we recursively perform the above steps, calculating the direction of the gradient until we find the source.

3.1 Gradient Estimation with Spatial Information

To exploit the spatial information in the signal field for gradient estimation, we are inspired by methods in previous studies [21, 28], in which the swarm robot team maintained a uniform, symmetrical circular formation to calculate the gradient. The uniform and symmetric distribution of circular formation make the sum of the vectors from each robot to the center of the circular formation a zero vector, which means

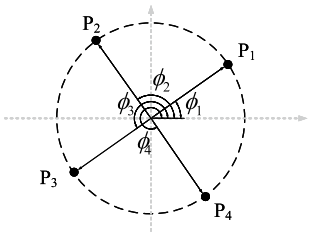

Fig. 2 The robots are evenly distributed in a circular formation

we could use the spatial information to estimate the gradient with the individual measurement of each robot.

We consider a robot team consisting of N robots, and they are organized in a circular formation. These N robots are evenly distributed on a circle with radius R, each of whose coordinates is represented as $p_i = (x_i, y_i)$, where x and y are respectively the abscissa and ordinate of robot i. A typical example is shown in Fig. 2, in which the number of agents N is set as 4. The agents in the team are uniformly distributed on a circle with a radius R and a center position of $c(x_c, y_c)$. Therefore, the ith robot among the evenly distributed agents could be observed as a position p_i in the circular formation, which could be formulated as follows:

$$p_i = c + R \cdot D(\phi_i) \tag{3}$$

where R is the radius of the circular formation, $D(\phi_i)$ is the direction function of the ith agent in the circular formation, where $\phi_i = \phi_0 + \frac{2\pi i}{N}$ represents the azimuth angle of the ith agent, which could be referred to Fig. 2. It could be easily obtained that $D(\phi_i) = (\cos\phi_i, \sin\phi_i)$.

All agents in this circular formation are fully-connected. The swarm agent team can approximate the signal field gradient through the weighted average of the signal strength collected by each individual agent [28], so as to achieve the purpose of spatial information fusion. Consider each agent measures the signal strength $z(p_i)$ at its current position $p_i(x_i, y_i)$ in the working space $\underline{W}$.

The length of each vector cP_i indicates the quantitative sampling value of each robot P_i. The sum of all corresponding vectors $\nabla z(c)$ indicates the final gradient estimation of the whole circular formation

Theorem 1 *The gradient direction of the circular formation center c is denoted as* $\nabla z(c)$, *which could be calculated by combining the measured values of multiple agents around the circular formation center c with a radius R*:

$$\frac{2}{NR^2}\sum_{i=1}^{N} z(p_i)(p_i - c) = \nabla z(c) + o(R) \tag{4}$$

where N is the number of agents in formation, and the approximation error term $o(R, c)$ *satisfies*:

$$\|o(R, c)\| \leq \lambda_{max}(H_z)R \tag{5}$$

where H_z *is the Hessian matrix of* $z(x)$, *and* $\lambda_{max}(x)$ *is the supremum of x, so* $\lambda_{max}(H_z)$ *is the supremum of the Hessian matrix* H_z.

Proof The reader are referred to [28] for details on the proof. □

As shown in Fig. 3, the gradient direction calculated by Eq. (4), incorporates the signal strength information of N agents at different spatial positions, so that the agent team can effectively estimate the gradient direction.

3.2 Gradient Estimation with Temporal Information

The above-mentioned gradient estimation method with circular formation makes full use of the spatial information in the cooperative network. To some extent, it can avoid the noise of individual source detection and improve source-seeking accuracy and robustness. However, existing studies, including the spatial fusion method in the above section, do not consider the time-series information. With this in mind, in this section, we proposed a virtual structure-based method to reduce the influence of noise on gradient estimation by introducing time-sequential information to the circular formation. Numerical simulations confirm the efficiency of the scheme put forth.

To integrate the temporal signal gradient and make the robot team find the source in the shortest distance with higher efficiency, the gradient is obtained by averaging the gradient in the target location and a nearby point. As the robot team moves, the target location enters the vision of the robot team. A circle with the target location as the center intersects the line segment formed by the target location and the previous round target location at one point. The robot team calculates the gradient when passing through this point. When the robot team arrives at the target location, the gradient is recalculated. The above two gradients are merged, which can be used as the gradient of the target location in the next step. The detailed process is described as shown in Fig. 4.

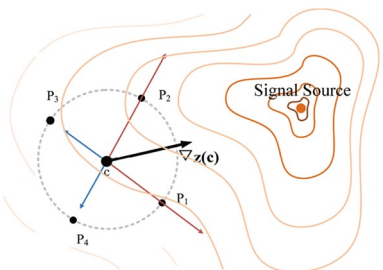

Fig. 3 Spatial gradient estimation of circular formations

In the k-th iteration, when the robot team calculates the target center position c_k of the symmetrical formation in this round, the robot team moves toward the target center position c_k. When c_k enters the field of vision of the robot team, let the circle centered on c_k and the expected vision radius d be circle C, take the point where the circle C and the line segment $c_k c_{k-1}$ intersect as c_{k-}.

When the robot team is moving towards the target location, the robot team passes through c_{k-} and c_k successively, and calculates the gradient when reaching these two points, and obtains the gradient $\nabla z(c_{k-})$ and $\nabla z(c_k)$.

The final gradient $\hat{g}_k$ of the robot team at c_k is obtained by calculating the weighted average of the above two gradients, and the next target location is calculated according to $\hat{g}_k$.

$$\hat{g}_k = \frac{1}{2}\left(\nabla z(c_{k-}) + \nabla z(c_k)\right) \tag{6}$$

Finally, the center position c_{k+1} of the circular agent team in $(k+1)th$ round is given by

$$c_{k+1} = c_k + a_k \hat{g}_k \tag{7}$$

where a_k is the step coefficient. The agent team continuously generates three series of points $\{c_{k-}, c_k\}$ through the above steps, and gradually moves to the vicinity of the signal source.

As for the step coefficient, it is generally denoted as

$$a_k = \frac{a}{(k+1+s)^{\alpha}}, \quad \text{k=0,1,...} \tag{8}$$

where a is a positive constant. s is a stability factor, which makes the algorithm have a large step size in the early iteration without causing instability, and should be set to 5% or 10% of the expected iterations of the algorithm. α controls the attenuation rate of the gain, and should be set to $\alpha = 0.602$, as suggested in [29].

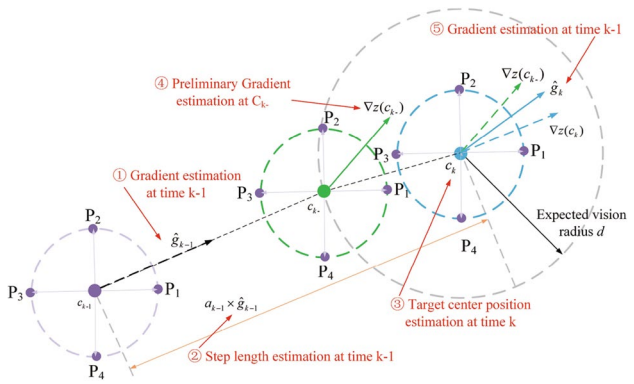

Fig. 4 An illustration of proposed cooperative source seeking method. It mainly contains the following five steps: (1) Perform spatial cooperative gratitude estimation at time $k-1$. (2) Calculate the step length using Eq. (10). (3) Further obtain the estimated target center position at time k using Eq. (8). (4) Obtain the preliminary gradient estimation at position c_{k-}. (5) Finally calculate the gradient estimation at time k

However, we need to modify a_k. Because if the numerator a is constant, the gain coefficient a_k decreases monotonically, which is not desirable. As the step length of the agent will gradually decrease, it may be trapped where the gradient estimation value is small. Our proposed method uses a variable instead, which is inversely proportional to the magnitude of the gradient estimate. When the gradient estimation value is large, the agent travels in smaller steps; if the magnitude of the gradient estimation decreases, the gain coefficient increases by increasing the step size. Even if the signal field is very flat, the agent can perceive the gradient by increasing the step size. According to the above principles, the expression of a_k is formulated as

$$a_k = \frac{\mathrm{r} \times (1+s)^{\alpha}}{\frac{1}{\zeta}\sum_{j=k-\zeta+1}^{k} \frac{1}{n}\left\|\hat{g}_j\right\|} \tag{9}$$

r is set as the greedy coefficient, the larger the value of r, the larger the step size coefficient of each step, and ζ is a coefficient that indicates the correlation between the current and the past gradients.

3.3 Control Strategy with Minimal Moving Cost

An algorithm based on gradient descent can drive the agent team to the target signal source position. However, without a good control strategy, the agents cannot use the gradient information. To more efficiently complete the source-seeking task, we propose a minimal moving distance control strategy.

During the movement of the agent team, the control strategy in this paper does not require the agent to maintain a fixed circular formation all the time. It aims to minimize the overall movement distance from the start point to the source. After the next formation center coordinates are calculated to achieve the control goal, the circular agent team can rotate an arbitrary angle around the formation center. Then we use optimization methods to find the angle that minimizes the moving distance.

We denote the distance that the ith agent need move from current position p_i to the next as $L(i) = \left\|p_i - p'_i\right\|$, where p'_i is the next step position of agent i. Our purpose is to minimize the overall moving cost of the agent team, so for the robot movement strategy we display as

$$L(\mathcal{P}) = \underset{p'_i \in \mathcal{P}}{arg\,min} \sum_{i}^{N} \left\|p_i - p'_i\right\| \tag{10}$$

where $\mathcal{P} = \{p'_1, ..., p'_N\}$. The overall cooperative source seeking method with applying the minimal moving cost control strategy could be seen in Algorithm 1.

Algorithm 1 Spatial-Temporal Cooperative Source Seeking

Input: initial position c_0, signal source position p_s
Output: final position c

Calculate the next position c_1 at initial position c_0 using (9), (11) and (10), then take the point where the c_1c_0 intersects the circle with d as the radius and c_1 as the center as c_{1-};
for $k = 1;\ \|p_k - p_s\| > 3;\ k++$ **do**
Move the agents to the position c_{k-} and c_k successively by optimizing (11), and then calculate the gradients $\nabla z(c_{k-})$ and $\nabla z(c_k)$;
Calculate calculate the next target position c_{k+1} using (8), (9) and (10);
Take the point where the $c_{k+1}c_k$ intersects the circle with d as the radius and c_{k+1} as the center as $c_{(k+1)-}$;
end for
Let $c \leftarrow c_k$;
return c

4 Theoretical Analysis

In this section, we detailed the importance of the proposed cooperative source-seeking method in theory. We firstly derived the Carmér-Rao Lower Bound (CRLB) [30] of gradient estimation error caused by the spatial–temporal fusion method. The lower bound of the proposed theoretical estimation accuracy is obtained. Then, the stability of the proposed algorithm is analyzed by Lyapunov inference [31].

4.1 Carmér-Rao Lower Bound

CRLB defines the theoretical lower limit of the variance of any unbiased estimator, which can be used as a benchmark for judgment and estimation methods. In this part, we analyze the CRLB of the variance of the gradient in the presence of control error.

Consider that each agent is able to measure the signal strength at its own position by $z(p_i)$ but the measurements are corrupted by white zero-mean Gaussian noise $\omega \sim \mathcal{N}(0, \sigma^2)$. Due to the noisy measurements, the weighted gradient estimation of the overall agent team should be bounded by:

$$E\left\{(z(c) - z(c))^2\right\} \geq CRLB = tr\left\{J^{-1}(z(c))\right\} \tag{11}$$

where $J(z(c))$ is the Fisher information matrix [30]. Then, with considering of Eq. (4), the denoted gradient estimation could be expressed as follows:

$$\frac{2}{NR^2}\sum_{i=1}^{N}(z(c) + \omega)(p_i - c) = \nabla z(c) + o(c) + o(R) \tag{12}$$

where $o(c)$ is the gradient estimation disturbance caused by the control error. Substitute Eqs. (4) into (12), we could obtain:

$$o(c) = \frac{2z(c)}{R^2}\omega \tag{13}$$

Thus, $o(c) \sim N(0, \frac{4|z(c)|^2\sigma^2}{R^4})$. Each estimated gradient $\hat{\nabla} z(c)$ is an estimator with Gaussian noise, namely $\hat{\nabla} z(c) \in N(\nabla z(c), \frac{4|z(c)|^2\sigma^2}{R^4})$. Then, the distribution function of $\hat{\nabla} z(c)$ is $f\left(\hat{\nabla} z(c)\right)$, and the Fisher information matrix function [30] could be denoted as:

$$J(\boldsymbol{p_i}) = -E\left[\frac{\partial \ln f}{\partial \nabla z(c)}\right]^2 = -\frac{R^4}{4|z(c)|^2\sigma^2} \tag{14}$$

Finally, the CRLB [30] of the weighted gradient estimation of the overall agent team could be derived as:

$$Var\left[\hat{\nabla} z(c) - \nabla z(c)\right] \geq tr\{J^{-1}(\boldsymbol{p_i})\} = \frac{4|z(c)|^2\sigma^2}{R^4} \tag{15}$$

The derived CRLB is proportional to the signal measurement noise variance and inversely proportional to the fourth power of the radius. Thus, given certain measurement conditions, the greater the radius, the smaller the influence of noise in the gradient approximation. However, as proven in Theorem 1, the error in the gradient approximation vanishes when the radius tends to zero.

For example, we set the signal strength $z(p)$ typically as $-$ 50 dB and the radius R of the symmetric formation to 1 m. Then, the CRLB estimation along with the noise standard deviation of ω is displayed in Fig. 5a. CRLB increases dispersedly with the increase of noise error, which indicates that the greater the measurement noise, the greater the error of the gradient estimation. On the other hand, we set the signal strength value $z(p)$ typically as $-$ 50 dB, and the standard deviation of signal measurement ω of the symmetric formation to 0.3 m. Then, the CRLB estimation along with the symmetrical formation radius R is displayed in Fig. 5b. The CRLB gradually decreases and slowly converges. However, it is not reasonable that R unrestrictedly increases in practice applications. Thus, we need to balance the value of radius R and improve the accuracy of gradient estimation by optimizing other parameters.

Consequently, we conclude that the radius of the robot team formation has an important role in gradient estimation and noise attenuation. How the formation radius affects the gradient estimation algorithm will be verified in the later numerical experiments.

4.2 Lyapunov Stability

We now prove the Lyapunov stability of the virtual structure-based method, which can prove that the method

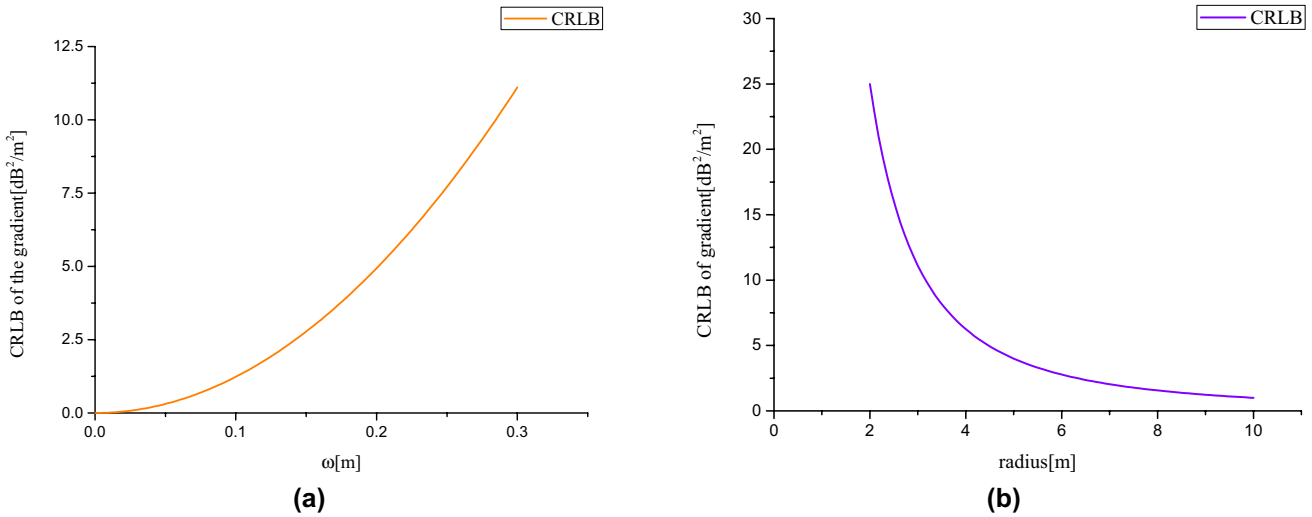

Fig. 5 Spatial performance evaluation based on the analysis of CRLB. **a** CRLB changing with standard deviation ω of the control error. **b** CRLB changing with the radius R of the symmetrical formation

proposed in this paper could ensure the robot team finally moves to the exact signal source in a scene where there is only one signal source without obstacles. We define the control law of the proposed source seeking method as:

$$\dot{c}_k = \mathbf{u} \tag{16}$$

where c_k is the center of agents' formation in the k-th iteration, and $\mathbf{u}$ is the control signal, it can be expressed as the following equation:

$$\mathbf{u} = a_k \frac{1}{2NR^2} \times \left(\sum_{i=1}^{N} z(p_i)(p_i - c) + \sum_{i=1}^{N} z(p_i^-)(p_i^- - c) \right) \tag{17}$$

where a_k is non-negative.

Theorem 2 *Assume that the signal strength is continuously derivable and satisfy the following property*:

$$\|c_1 - p_s\|_2 < \|c_2 - p_s\|_2 \Rightarrow z(c_1) > z(c_2) \tag{18}$$

which shows that it has a maximum value at p_s, and the signal strength decreases as the Euclidean distance from p_s increases. Under the control law of (16)*, the point of p_s is an asymptotically stable equilibrium in the cooperative source seeking method.*

Proof We construct the Lyapunov function [31] as follow:

$$V(c_k) = z(p_s) - z(c_k) \tag{19}$$

which is zero at $c_k = p_s$ and positive otherwise. The time derivative of (19) is:

$$\dot{V}(c_k) = -\nabla z(c_k)^{\mathrm{T}} \dot{c}_k \tag{20}$$

Substitute Eq. (17) into the above equation to get:

$$\dot{V}(c_k) = -\nabla z(c_k)^{\mathrm{T}} a_k \frac{1}{2NR^2} \times \left(\sum_{i=1}^{N} z(p_i)(p_i - c) + \sum_{i=1}^{N} z(p_i^-)(p_i^- - c) \right) \tag{21}$$

where the gradient $\nabla z(c_k)$ can be expressed as follow:

$$\nabla z(c_k) = \mu \frac{c_k - p_s}{\|c_k - p_s\|_2} \tag{22}$$

where μ is a coefficient related to the gradient size. It is obvious that $\nabla z(c_k)$ is a vector from c_k to p_s. According to our definition of the field strength function $z(c)$, the coefficient μ satisfies the following conditions:

$$\mu \geq 0 \tag{23}$$

By substituting the definition of $\nabla z(c_k)$ into $\dot{V}(c_k)$, we get:

$$\dot{V}(c_k) = -a_k \frac{\mu}{\|c_k - p_s\|_2} \frac{1}{NR^2} \times \left(\sum_{i=1}^{N} z(p_i)(c_k - p_s)^{\mathrm{T}}(p_i - c) + \sum_{i=1}^{N} z(p_i^-)(c_k - p_s)^{\mathrm{T}}(p_i^- - c) \right) \tag{24}$$

where a_k is positive, $\frac{\mu}{\|c_k-p_s\|_2}$ is non-negative, $\frac{1}{NR^2}$ is non-negative. To determine the lower bound of $\dot{V}(c_k)$, we introduce a set that changes over time:

$$\mathcal{M} = \{p_i : (c_k - p_s)^{\mathrm{T}}(p_i - c) > 0\} \tag{25}$$

Thus, the cumulative sum in $\dot{V}(c_k)$ can be expressed in the following form:

$$\begin{aligned}\dot{V}(c_k) = &- a_k \frac{\mu}{\|c_k - p_s\|_2} \frac{1}{NR^2} \times \\ &\left(\sum_{p_i \in \mathcal{M}} z(p_i)(c_k - p_s)^{\mathrm{T}}(p_i - c) + \right. \\ &\left. \sum_{p_i \notin \mathcal{M}} z(p_i)(c_k - p_s)^{\mathrm{T}}(p_i - c) \right)\end{aligned} \tag{26}$$

It is easy to know that if $c_k \neq p_s$, then those agents in $\mathcal{M}$ are all closer to the source p_s than those agents not in $\mathcal{M}$ (for example, $\mathcal{M} = \{p_1, p_2, p_{1-}, p_{2-}\}$ in Fig. 4). Because the signal strength measured by the robot closer to ps is greater, for all p_k and p_m:

$$p_k \in \mathcal{M}, p_m \notin \mathcal{M}, \exists \delta > 0 \tag{27}$$

then we get:

$$z(p_k) > \delta > z(p_m) \tag{28}$$

If we apply the above inequality to the sum of the above equation, we get:

$$p_i \in \mathcal{M} \Rightarrow \underbrace{z(p_i)}_{>\delta} \underbrace{(c_k - p_s)^{\mathrm{T}}(p_i - c)}_{>0} > \delta(c_k - p_s)^{\mathrm{T}}(p_i - c) \tag{29}$$

and

$$p_i \notin \mathcal{M} \Rightarrow \underbrace{z(p_i)}_{<\delta} \underbrace{(c_k - p_s)^{\mathrm{T}}(p_i - c)}_{\leq 0} \geq \delta(c_k - p_s)^{\mathrm{T}}(p_i - c) \tag{30}$$

We assume that $\mathcal{M}$ is not an empty set (that is always true when N>2), and that the sum in $\mathcal{M}$ is bounded by:

$$\begin{aligned}&\sum_{p_i \in \mathcal{M}} z(p_i)(c_k - p_s)^{\mathrm{T}}(p_i - c) + \sum_{p_i \notin \mathcal{M}} z(p_i)(c_k - p_s)^{\mathrm{T}}(p_i - c) \\ &> \delta(c_k - p_s)^{\mathrm{T}} \sum_{k=1}^{N} (p_i - c)\end{aligned} \tag{31}$$

The agents are uniformly distributed in a circular formation, so $\sum_{k=1}^{N} (p_i - c) = 0$. $a_k > 0$ and $\frac{\mu}{\|c_k-p_s\|_2}$ is non-negative. From the above conditions we get: when $\mathcal{M}$ is not an empty set, $\dot{V}(c_k) < 0$ is true for all $c_k \neq p_s$. According to the LaSalle's invariant set principle [31], the point p_s is asymptotically stable under the control law (13).

□

With the above derivation of the Lyapunov equation, it is proved that our proposed method can converge to the optimal solution.

5 Numerical Simulation and Discussion

To verify the effectiveness, we compared our proposed method with two state-of-the-arts [21, 28] in the numerical experiments. The method in [21] has only one robot for the source seeking task, while the method in [28] presented a circular team of four agents for source seeking. Besides, two scenarios are set up in this paper, one is a single-source scenario, and the other is a local optimal dual-source scenario.

5.1 Experiment Setup

A scalar signal source simulates a working space W with the coordinates of signal source $p_s = (5m, 25m)$. The collective information, as well as signal strength in this experiment, received by each agent in the working space, is given by the following equations. The overall signal source model used in the experiment is denoted as follows [28]:

$$z(p) = -20.05 - 20\log_{10}\|p - p_s\| - N \tag{32}$$

where p is the current position of the robot, p_s is the position of the signal source, and N is the signal noise. Thereinto, $N = \sqrt{\alpha^2 + \beta^2}$. α and β both have normal distributions respectively, where $\alpha \sim \mathcal{N}(\nu \cos\theta, \sigma^2)$, $\beta \sim \mathcal{N}(\nu \sin\theta, \sigma^2)$, and σ is the standard deviation, ν and θ both influence the mean of the distribution. The initial position of the robot team center is $p_{init} = (25m, 5m)$. This article conducts verification and analysis under the above experimental conditions. In the following part, we compare the method proposed in this article with state-of-the-arts in [21] and [28]. Numerical simulations confirm the efficiency of the scheme put forth.

5.2 Typical Experimental Results in Single Source

We chose the first experimental scenario, the signal field used is given by Eq. (32). For the noise term N, we set the parameters as ν=2, θ=$\frac{\pi}{3}$, σ=1. These parameters are used to generate the experimental signal field. Two comparative methods and our own proposed one are performed 100 times in the same experimental scenario. When the distance

between the source and the agent's center approaches 0, we take it as the agents in formation successfully find the source. The speed of finding signal sources is one of the important indicators to measure the algorithm's efficiency. The fewer iteration steps that the agents take to reach the signal source, the faster the distance converges to zero and the higher the algorithm's efficiency.

A typical numerical simulation is displayed in Fig. 6, from which we could conclude that the two comparative methods are more easily affected by signal noises, as their trajectories (green and magenta ones) fluctuated more heavily and are more tortuous. In contrast, the trajectory curve obtained by the method described in this paper (the red one) is smoother and simpler, which implicit that our approach is more efficient and robust to various changing signals. The method proposed in this paper reduces the interference of noise on the gradient calculation. It makes the trajectory more consistent with the direction of the gradient increase in the signal field. This shows that our proposed virtual structure-based method has better stability and anti-noise characteristics.

Furthermore, the averages of 100 experimental results are taken as the final experimental output. The variance of calculated total movement distances is drawn as error bars in Fig. 7, demonstrating the detailed tendency of distance variance along with the iteration steps. Fig. 7 shows the distance between the current agent formation center and the signal source, along with the number of iteration steps. It can be seen that our proposed spatial–temporal cooperative source-seeking method convergences faster than comparative methods. The circular formation method that is superior to the [28] is also far superior to the random approximation method of [21], indicating that the cooperative estimation among agents outperforms independent work and could solve the source seeking problem more efficiently. In addition, the numerical results are demonstrated in Table 1.

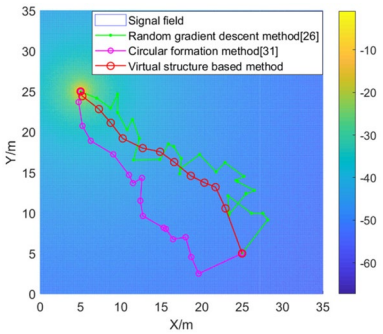

Fig. 6 Comparison of trajectories of proposed method and state-of-the-arts

5.3 Cumulative Distances with Noise Variance

The cumulative distances represent the total movement distances made by each agent, traveling from the starting position to the signal source. The smaller the cumulative distances, the source seeking method is more efficient.

The control variable of this experiment is the noise variance of the signal field, that is, the noise term N in Eq. (32). We vary the noise variance of the signal field and then compare the differences of the cumulative distances of the agents calculated by the three different source-seeking methods. Let $\sigma=\{1, 1.5, 2, 2.5, 3, 3.5, 4, 4.5, 5, 5.5\}$. In different signal fields generated by different noise parameters σ, we performed three algorithms 100 times in various signal fields and then recorded the averages and variances of each experiment.

Figure 8 shows the robot's cumulative distances of all three methods as the noise variance of σ changes. The

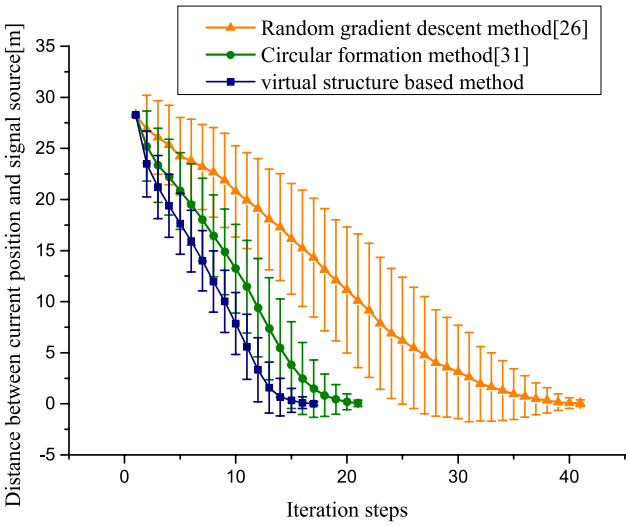

Fig. 7 The distance from the center of the robot to the source varies with the number of iteration steps

Table 1 The distance between formated team center and the signal source changes with the iteration steps with use of different methods

Distance to the source/*m*									
Iteration steps	1	6	11	16	21	26	31	36	41
Method in [28]	28.28	22.99	18.01	11.07	3.45	0.21	0	0	0
Method in [21]	28.28	23.79	19.90	15.21	10.09	5.47	2.61	0.72	0.05
Proposed method	28.28	22.72	15.98	7.03	0.73	0	0	0	0

variance of 100 experimental results gives the error bars in the figure. It can be seen from Fig. 8 that our proposed spatial–temporal cooperative source seeking method has significantly smaller cumulative distances than those of [21], and [28] under the same noise condition. The proposed cooperative source seeking method enables the agents to find the signal source with a shorter movement distance and higher search efficiency. Quantitatively, we display the results of the numerical experiment in Table 2.

On the other hand, as the noise variance σ increases, the curves of the three methods all have an upward tendency. The growth rate of the proposed spatial–temporal cooperative source seeking method is significantly lower than those of other comparative algorithms, and the gap with the other two is getting wider and wider. It indicates that the proposed method is significantly more robust to noise interference than the methods in [21] and [28]. In addition, the amplitude of the error bars of the proposed method is also smaller, which means more stable and robust to noise characteristics.

5.4 Cumulative Distances with Various *R*

As we declared in Sect. 4.1, the formation radius R has an important role in the gradient estimation and the noise attenuation. The gradient estimation variance is inversely proportional to the radius squared; thus, the greater the radius, the smaller the influence of noise in the gradient approximation. As proven in Theorem 1, the error in the gradient approximation vanishes when the formation radius R tends to zero. However, larger R can also contribute to the information gathering and finally lead to a smaller accumulative distance of the overall source-seeking process. We carried out numerical simulation experiments for the source-seeking process with various formation radius to further quantitatively evaluate the influence of formation radius on the accumulative distance.

From Fig. 9 we can conclude that with a larger radius, the formated agents could achieve the source with smaller accumulative distances and smaller variance with the use of our proposed spatial–temporal method. Our explanation for this is that a larger radius introduces more spatial information to the algorithm, and in the meantime, improves the stability of the system as a whole. However, the formation radius is not as larger as better, owing to communication and monitoring area constraints. Everything is taken into account. The radius chosen as 1 to 2 m is generally appropriate based on our close attempts.

5.5 Typical Experimental Results in Multiple Sources

We added a new signal source in the multiple sources scenario whose signal strength is half of the original

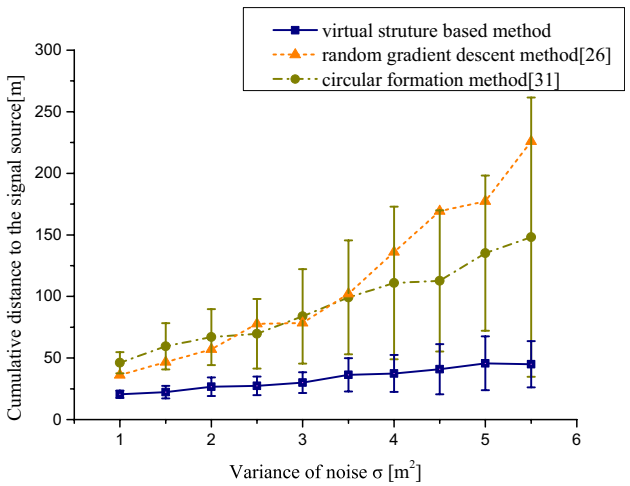

Fig. 8 Cumulative distance changes with noise variance σ

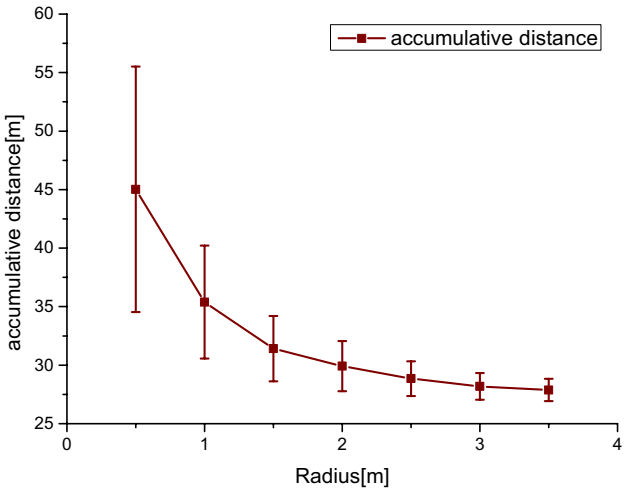

Fig. 9 Cumulative distance changes with various formation radius R

Table 2 The cumulative distance changes with various variances with use of different methods

Cumulative distances/*m*									
Noise variance/m^2	1.0	1.5	2.0	2.5	3.0	3.5	4.0	4.5	5.0
Method in [28]	49.67	56.16	59.84	68.09	76.43	81.77	87.90	100.49	109.53
Method in [21]	36.22	46.68	57.01	77.75	78.46	102.10	136.07	169.29	177.22
Proposed method	31.81	36.07	40.03	44.67	51.03	55.61	53.80	66.68	73.20

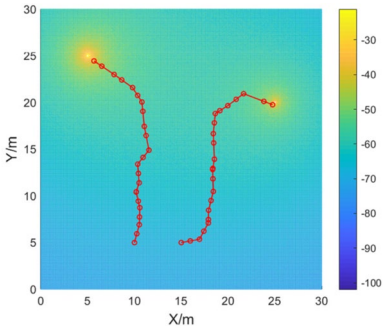

Fig. 10 The typical trajectory of the robot team in the presence of local optimal values, with different initial positions

signal source. Its position p'_s is between the robot's starting position and the first signal source position p_s, and $p'_s = (20m, 20m)$, we will conduct experiments in this scenario and show typical experimental results.

$$z(p) = -20.05 - 20\log_{10}\|p - p_s\| - 10\log_{10}\|p - p'_s\| - N \tag{33}$$

In the scenario where two signal sources exist, we conducted 100 experiments. In each experiment, the robot team moved to the vicinity of the second signal source p'_s. We drew the trajectory of the typical robot team in the experiment in Fig. 10. Then, we can see that the robot team has found the location of the second signal source p'_s, which shows that our proposed method can find the local optimal value according to the gradient of the signal field. In multiple sources, the agents converge to a local maximum depending on their initial conditions. For each simulation, the initial conditions are different to show the local stability properties of our approach. In both conditions, the agents converge to a local maximum depending on their initial conditions. As shown in Fig. 10, the convergence rate also depends on the initial conditions and the shape of the signal measured.

6 Conclusions

This paper proposed a spatial–temporal method for multi-robot cooperative sources seeking to fuse spatial and temporal information in the scalar field. With the derivation of the CRLB and Lyapunov equation, it is proved that our proposed method can converge to the optimal solution and be bounded by certain error limits. Compared with state-of-the-art multi-robot collaborative methods, our proposed method enables the robots to find signal sources with smaller iteration steps and cumulative distances, effectively reducing task overhead and improving efficiency. Our future work will focus on reducing the formation error of the robot team, which may provide a more accurate gradient estimation with circular or arbitrary formation for better facilitation of practical applications.

Acknowledgements This work is supported in part by China National Postdoctoral Program for Innovative Talents under Grant BX20190033, in part by Guangdong Basic and Applied Basic Research Foundation under Grant 2019A1515110325, in part by Project funded by China Postdoctoral Science Foundation under Grant 2020M670135, in part by Postdoctor Research Foundation of Shunde Graduate School of University of Science and Technology Beijing under Grant 2020BH001, and in part by the Fundamental Research Funds for the Central Universities under Grant 06500127.

Data Availability All related simulation data will be made available upon reasonable request from the corresponding authors (C. Xu and S. Duan) for academic use and within the limitations of the provided informed consent by the corresponding author upon acceptance.

References

1. D. Waleed et al., "An In-Pipe Leak Detection Robot With a Neural-Network-Based Leak Verification System," in IEEE Sensors Journal, vol. 19, no. 3, pp. 1153-1165, 1 Feb.1, 2019.
2. H. Che, C. Shi, X. Xu, J. Li and B. Wu, "Research on Improved ACO Algorithm-Based Multi-Robot Odor Source Localization," 2018 2nd International Conference on Robotics and Automation Sciences (ICRAS), Wuhan, 2018, pp. 1-5.
3. X. Cao, Z. Jin, C. Wang and M. Dong, "Kinematics simulation of environmental parameter monitor robot used in coalmine underground," 2016 13th International Conference on Ubiquitous Robots and Ambient Intelligence (URAI), Xi'an, 2016, pp. 576-581.
4. Li, Zhuo, Keyou You, and Shiji Song. "Cooperative source seeking via networked multi-vehicle systems." Automatica 115 (2020): 108853.
5. M. Kanwar and L. Agilandeeswari, "IOT Based Fire Fighting Robot," 2018 7th International Conference on Reliability, Infocom Technologies and Optimization (Trends and Future Directions) (ICRITO), Noida, India, 2018, pp. 718-723.
6. Consi, T. R., et al. "AUV guidance with chemical signals." Proceedings of IEEE Symposium on Autonomous Underwater Vehicle Technology (AUV'94). IEEE, 1994.
7. Chen, Xin-xing, and Jian Huang. "Odor source localization algorithms on mobile robots: A review and future outlook." Robotics and Autonomous Systems 112 (2019): 123–136.
8. Russell, R. Andrew, et al. "A comparison of reactive robot chemotaxis algorithms." Robotics and Autonomous Systems 45.2 (2003): 83-97.
9. M. Dorigo, V. Maniezzo and A. Colorni, "Ant system: optimization by a colony of cooperating agents," in IEEE Transactions on Systems, Man, and Cybernetics, Part B (Cybernetics), vol. 26, no. 1, pp. 29–41, Feb. 1996.
10. D. Karaboga, An idea based on honeybee swarm for numerical optimization, Technical Report TR06, Erciyes University, Engineering Faculty, Computer Engineering Department, 2005.
11. Cai, Y. and Y. Shen, An Integrated Localization and Control Framework for Multi-Agent Formation. IEEE Transactions on Signal Processing, 2019. 67(7): p. 1941–1956.
12. Neto, Mário Tasso Ribeiro Serra, Marco Antônio Florenzano Mollinetti, and Rodrigo Lisbôa Pereira. "Evolutionary artificial bee colony for neural networks training." 2017 13th International

Conference on Natural Computation, Fuzzy Systems and Knowledge Discovery (ICNC-FSKD). IEEE, 2017.
13. W. Wu and F. Zhang, "A Speeding-Up and Slowing-Down Strategy for Distributed Source Seeking With Robustness Analysis," in IEEE Transactions on Control of Network Systems, vol. 3, no. 3, pp. 231–240, Sept. 2016.
14. S. Al-Abri, W. Wu and F. Zhang, "A Gradient-Free Three-Dimensional Source Seeking Strategy With Robustness Analysis," in IEEE Transactions on Automatic Control, vol. 64, no. 8, pp. 3439–3446, Aug. 2019.
15. J. Kennedy and R. Eberhart, "Particle swarm optimization," Proceedings of ICNN'95 - International Conference on Neural Networks, Perth, WA, Australia, 1995, pp. 1942-1948 vol.4.
16. Jatmiko, Wisnu, Kosuke Sekiyama, and Toshio Fukuda. "A pso-based mobile robot for odor source localization in dynamic advection-diffusion with obstacles environment: theory, simulation and measurement." IEEE Computational Intelligence Magazine 2.2 (2007): 37–51.
17. Jatmiko, Wisnu, et al. "Robots implementation for odor source localization using PSO algorithm." WSEAS Transactions on Circuits and Systems 10.4 (2011): 115-125.
18. Song, C., L. Liu and S. Xu, Circle Formation Control of Mobile Agents With Limited Interaction Range. IEEE Transactions on Automatic Control, 2019. 64(5): p. 2115–2121.
19. Yang, Linyu, and Shujun Liu. "Distributed Stochastic Source Seeking for Multiple Vehicles over Fixed Topology." Journal of Systems Science and Complexity 33.3 (2020): 652–671.
20. Song, Cheng, et al. "Collaborative infotaxis: Searching for a signal-emitting source based on particle filter and Gaussian fitting." Robotics and Autonomous Systems 125 (2020): 103414.
21. N. Atanasov, J. Le Ny, N. Michael and G. J. Pappas, "Stochastic source seeking in complex environments," 2012 IEEE International Conference on Robotics and Automation, Saint Paul, MN, 2012, pp. 3013-3018.
22. P. Ögren, E. Fiorelli and N. E. Leonard, "Cooperative control of mobile sensor networks: Adaptive gradient climbing in a distributed environment," in IEEE Transactions on Automatic Control, vol. 49, no. 8, pp. 1292–1302, Aug. 2004.
23. Zhu S, Wang D, Low C B. Cooperative control of multiple UAVs for moving source seeking[J]. Journal of Intelligent & Robotic Systems, 2014, 74(1–2): 333–346.
24. S. Li, R. Kong and Y. Guo, "Cooperative Distributed Source Seeking by Multiple Robots: Algorithms and Experiments," in IEEE/ASME Transactions on Mechatronics, vol. 19, no. 6, pp. 1810–1820, Dec. 2014.
25. R. Fabbiano, F. Garin and C. Canudas-de-Wit, "Distributed Source Seeking Without Global Position Information," in IEEE Transactions on Control of Network Systems, vol. 5, no. 1, pp. 228–238, March 2018.
26. Briñón-Arranz L, Seuret A, Pascoal A. Circular formation control for cooperative target tracking with limited information[J]. Journal of the Franklin Institute, 2019, 356(4): 1771–1788.
27. Silic, Matthew, and Kamran Mohseni. "Field deployment of a plume monitoring UAV flock." IEEE Robotics and Automation Letters 4.2 (2019): 769–775.
28. Briñón-Arranz, Lara, Alessandro Renzaglia, and Luca Schenato. "Multirobot Symmetric Formations for Gradient and Hessian Estimation With Application to Source Seeking." IEEE Transactions on Robotics 35.3 (2019): 782–789.
29. J. Spall, Intro to Stochastic Search and Optimization. Wiley, 2003.
30. Xu C, He J, Zhang X, et al. Toward near-ground localization: Modeling and applications for TOA ranging error[J]. IEEE Transactions on Antennas and Propagation, 2017, 65(10): 5658–5662.
31. Sastry S. Nonlinear systems: analysis, stability, and control[M]. Springer Science & Business Media, 2013

Cheng Xu received the B.E., M.S. and Ph.D. degree from the University of Science and Technology Beijing (USTB), China in 2012, 2015 and 2019 respectively. He is currently working as an associate professor in the Data and Cyber-Physical System Lab (DCPS) at University of Science and Technology Beijing. He is supported by the Post-doctoral Innovative Talent Support Program from Chinese government in 2019. He is an associate editor of International Journal of Wireless Information Networks. His research interests now include swarm intelligence, multi-robots network, wireless localization and internet of things. He is a member of the IEEE.

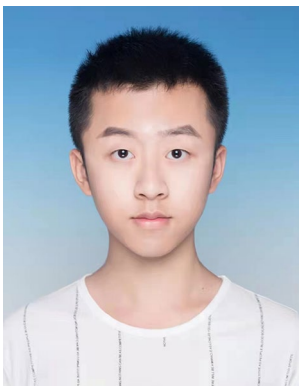

Jiawei Rong is working toward the Bachelor degree at University of Science and Technology Beijing, China. His research interests include multi-robot system and reinforcement learning.

Yulin Chen got the Master degree at University of Science and Technology Beijing, China in 2021. His research interests include patter recognition and internet of things.

Hang Wu is currently working toward the Master degree at University of Science and Technology Beijing. Her research interests include patter recognition and internet of things.

Shihong Duan received Ph.D. degree in computer science from University of Science and Technology Beijing (USTB). She is an associate professor with the School of Computer and Communication Engineering, USTB. Her research interests includes wireless indoor positioning, human gesture recognition and motion capture.